Med Chem Res (2013) 22:2862–2869
DOI 10.1007/s00044-012-0286-5

MEDICINAL CHEMISTRY RESEARCH

ORIGINAL RESEARCH

Synthesis, characterization, and antitumor activity of rare earth metal complexes of benzoic acid nitrogen mustard

Sufeng Zhou · Yun Fu · Xizhi Fan · Yanfang Zhang · Changzheng Li

Received: 21 March 2012 / Accepted: 20 October 2012 / Published online: 2 November 2012

Abstract Benzoic acid nitrogen mustard and its rare earth metal complexes were synthesized and characterized by elemental analyses, IR, electronic spectrum, and EPR. The interaction of synthesized complexes with Ct-DNA was investigated and reviewed as a mixed manner of both intercalation and alkylation via fluorescence titration. Their biological activities were also evaluated in K_{562} and Vero cell lines, indicating that complexes had a significant inhibitory effect; however, there was no synergistic effect instead of antagonistic effect compared to benzoic acid nitrogen mustard. The possible mechanism through cellular apoptosis was also explored by comet assay.

Keywords Benzoic acid nitrogen mustard · Synthesis · Antitumor activity · Rare earth metal complex · Comet assay

Introduction

Nitrogen mustard is one of the most useful drugs in cancer chemotherapy, lack of selectivity and its toxic-side effect as well as resulting drug-resistance, carcinogenesis, and mutation, make its applications limited. In order to improve its antitumor activity, many of its derivatives have been synthesized; melphalan, cyclophosphamide, bendamustine, and chlorambucil are good examples and have been widely used in clinic (Leoni *et al*., 2008). Among massive derivatives of nitrogen mustard, benzoic acid nitrogen mustard (BANM) is effective against quiescent cell and tend to be less susceptible to induced resistance than most anticancer drugs, thereby its different derivatives were reported in many literatures (Beria and Nesi, 2002; Koutsourea *et al*., 2008). In addition to its good fluorescence and noncell-cycle-specific feature, BANM is widely used in prodrug design (Roger and Roger, 1996), such as antibody-directed enzyme prodrug therapy, which is designed to deliver it to a given site.

It is well known that rare earth metal is an important chemical element and has significant biological feature. Rare earth metal complexes have been widely used as diagnosis reagent for pathological changes of lung, brain, and kidney (Zhou *et al*., 2010). Some complex has ability to promote blood circulation and protect cells from radiation damage (Gschneidner *et al*., 1999). In addition, the rare earth metal complexes have not been shown to have a cumulative effect in vivo either as a result of oral administration or external use (Li *et al*., 2011). Their anti-inflammation and anticancer activity indicate that rare earth ions can stop bacterium metabolism (Qu *et al*., 2006) or inhibit enzymatic activity (Achyuthan *et al*., 1989). However, the complexes of rare earth with BANM are not reported in literature. In order to evaluate whether a synergistic effect exists between them, BANM was synthesized by multi-step and its rare earth complexes were also prepared. Their biological activities were evaluated against Vero and K_{562} cell lines, and the interactions with Ct-DNA and cellular DNA in vitro were examined to probe their interaction and the underlying biological mechanism.

Y. Fu · Y. Zhang · C. Li (✉)
Department of Molecular Biology & Biochemistry, Xinxiang Medical University, Xinxiang 453003, Henan, People's Republic of China
e-mail: changzhenl@yahoo.com

S. Zhou
Clinical Skill Training Center, Xinxiang Medical University, Xinxiang 453003, Henan, People's Republic of China

X. Fan
Department of Computer, Xinxiang Medical University, Xinxiang 453003, Henan, People's Republic of China

Experimental

All reactants and solvents were AR grade. 3-(4,5-Dimethylthiazol-2-yl)-2,5-diphenyltetrazolium bromide (MTT), sodium dodecyl sulfate (SDS), ethidium bromide (EB), Roswell Park Memorial Institute 1640 (RPMI-1640), and agarose were purchased from Sigma. Calf thymus DNA (Ct-DNA) was obtained from Shanghai Lizhu Dong Feng Biotechnology Co. LTD, Shanghai.

Instrumentation and measurement

Stock solutions of nucleic acids were prepared by directly dissolving commercial Ct-DNA in ddH_2O, and the resulting solution was subjected to dialysis in the ddH_2O at 4 °C. The Ct-DNA sample purity was estimated by measurement of A_{260} and A_{280}; the ratio A_{260}/A_{280} was above 1.8, indicating that the nucleic acid was reasonably free of protein contamination (Nelson and Cox, 2004). The molar concentration of Ct-DNA was calculated according to the following formula:

$C_{DNA} = KA_{260}/6{,}600$, here K is the dilution factor.

The solutions of complexes (5.0×10^{-4} M) were prepared by dissolving them in DMSO-ethanol mixture solvent (1:10, v/v).

Nitrogen, carbon, and hydrogen were determined using an Elementar Vario EL. The IR spectra were recorded in the 4,000–200 cm^{-1} region using KBr pellets and a Nicolet-170-SX FTIR spectrometer. Electronic spectra in DMSO were measured on a Shimadzu UV-240 spectrophotometer. Conductance measurement was carried out with a DDS-11A type conductivity bridge in DMSO at 10^{-3} M. EPR spectra (in solid and solution states) were obtained from Bruker ER200D-SRC instrument at room temperature. The magnetic field was varied from 0 to 6800 Gs. The spectra of fluorescence were recorded on Hitachi 850 fluorescent spectrophotometer. Thermogravimetric analysis (TG) and differential thermal analysis (DTA) was carried out using a diamond TG/DTA instrument (PerkinElmer). Isothermally heated to 30 °C for 10 min under air flow (200 ml/min) and then heated from 30 to 800 °C in a static air atmosphere. The heating rate was 10 °C/min. Al_2O_3 was used as the reference standard.

Preparation of benzoic acid nitrogen mustard

The synthetic scheme of BANM was as follows (Fig. 1):

4,4-Bis(2-chloroethyl)amino-benzaldehyde (benzaldehyde nitrogen mustard) was made according to our published method (Li *et al*., 1999). BANM was prepared by $KMnO_4$ oxidation of benzaldehyde nitrogen mustard.

Preparation of the complexes

In a typical preparation, a solution of hydrated lanthanide acetate (77.8 mg, 0.2 mmol) in 50 % water–ethanol was added dropwise to a solution of BANM (78.7 mg, 0.6 mmol) in 10 ml ethanol with stirring, the precipitate was formed. The mixture was continuously stirred for 8 h. The product was filtered off, washed with 50 % aqueous-ethanol, and dried in vacua. The yield was ~80 %. The analytical data of BANM and the complexes are presented in Table 1.

Fluorescence studies

The Scatchard plots were generated using following procedure: in a 5-ml volumetric flask, 0.5 ml of Ct-DNA (1.5×10^{-5} M), 2.0 ml Tris–HCl buffer (pH 7.2), 0.5 ml NaCl (0.5 M), and the solution of complexes with different molar ratio ($R_t = C_{complex}/C_{DNA}$) were added. After diluted to 5 ml, the mixture was then titrated by 0.1 mg/ml EB solution. The fluorescence intensity was determined at $\lambda_{ex}/\lambda_{em} = 525/600$ nm.

The effects of the complexes on the fluorescence spectrum of Ct-DNA-EB was evaluated based on the following method: 0.5 ml of 50 μM Ct-DNA, 0.5 ml of 10 μM EB, 0.5 ml of 0.5 M NaCl, 2.0 ml Tris–HCl buffer (pH 7.2), and an appropriate amount of Ln(III) complexes were mixed in a 5-ml volumetric flask and diluted to the giving volume with ddH_2O. The fluorescence intensity was determined at $\lambda_{ex}/\lambda_{em} = 525/600$ nm.

MTT assay

The stock solutions of BANM complex were freshly prepared in 10 % DMSO, and were diluted to the required concentration with culture when used. Vero (African green monkey kidney cell) and K_{562} human leukemia cells were

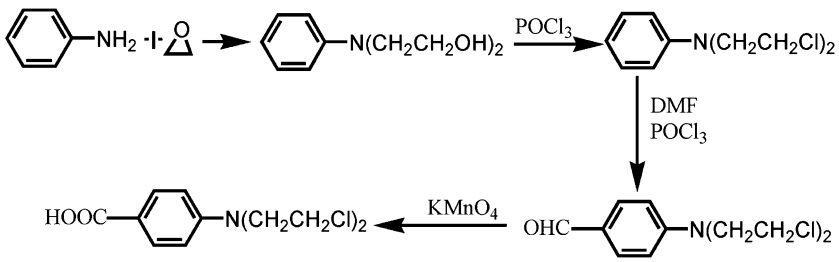

Fig. 1 Synthetic routes of benzoic acid nitrogen mustard

Table 1 Analytical data and general appearance of Ln(III) complexes

Compound	Color	Percent composition (%) found (calc.)			
		C	N	H	M
BANM	Colorless	50.1 (50.4)	5.7 (5.3)	4.8 (5.0)	
$La(BANM)_3H_2O$	White	41.9 (42.2)	4.4 (4.5)	4.2 (4.1)	15.2 (14.8)
$Nd(BANM)_3H_2O$	Slight blue	41.6 (41.9)	4.6 (4.4)	4.3 (4.1)	15.6 (15.3)
$Sm(BANM)_3H_2O$	White	42.0 (41.6)	4.6 (4.4)	4.5 (4.0)	16.1 (15.8)
$Eu(BANM)_3H_2O$	Pale yellow	42.0 (41.6)	4.5 (4.9)	4.5 (4.0)	16.3 (15.9)
$Gd(BANM)_3H_2O$	White	41.9 (41.4)	4.8 (4.4)	4.3 (4.0)	16.0 (16.4)
$Dy(BANM)_3H_2O$	Pale yellow	41.0 (41.1)	4.7 (4.4)	3.9 (4.0)	17.1 (16.9)
$Er(BANM)_3H_2O$	Slight red	41.2 (40.9)	4.7 (4.3)	4.2 (4.0)	17.1 (17.3)
$Tm(BANM)_3H_2O$	Slight red	40.6 (40.9)	4.7 (4.3)	4.0 (4.0)	17.8 (17.4)

propagated continuously in RPMI 1640 medium supplemented with 10 % freshly inactivated fetal calf serum (FCS) and antibiotics. The cells harvested from exponential phase (2×10^5/ml) were seeded equivalently into 96-well plate and the compounds studied were added in varied concentrations. The plate was kept at 37 °C in a humidified atmosphere of 5 % CO_2 for 48 h, MTT solution of an appropriate concentration (1 mg/ml) was added to each well, and the plate was further incubated at 37 °C for 4 h. Finally, 100 µl of 10 % SDS solution containing 1 % HCl was added to each well and the plate was kept at 37 °C for overnight. The measurement of absorbencies was performed on an ELISA spectrophotometer at 570 nm.

Comet assay

The single-cell gel electrophoresis (comet assay) was adapted from the method of Singh and colleagues reported in reference (Singh *et al*., 1988). K_{562} cells treated with (50 µM) or without of lanthanide BANM after 48 h incubation in a humidified atmosphere of 5 % CO_2 were harvested by centrifugation at 1,000 rpm and then embedded in 0.5 % low-melting-point agarose at a final concentration of 10^4 cells/ml. 20 µl of this cellular suspension was then spread onto duplicate frosted slides that had previously been covered with 1 % normal-melting-point agarose as a basal layer. Slides were allowed to solidify for 10 min at 4 °C before being placed in lysis buffer for 1 h (2.5 M NaCl, 0.1 M ethylene diamine tetraacetic acid (EDTA), 0.01 M Tris, 1 % Triton X-1000, 10 % dimethyl sulphoxide (DMSO), pH 10). After lysis, the slides were transferred into alkaline buffer for 40 min (0.001 M EDTA, 0.3 M NaOH, pH >13) to allow the DNA to unwind before migration at 0.66 V/cm and 300 mA for 30 min. All these steps were performed in the dark. After neutralization in 0.4 M Tris–HCl pH 7.4, slides were stored at 4 °C until analysis during the following 24 h period. Before analysis, the slides were stained with EB (20 µg/ml) and covered with a cover-slip. The photography was taken on fluorescent microscopy.

Results and discussion

Characterization of the complexes

An Elementar Vario EL elemental analyzer was used to analyze the carbon, hydrogen, and nitrogen content of BANM and its complexes. The metal content was determined by EDTA complexometric titration. As presented in Table 1, the composition of the complexes were found to be 1:3 stoichiometry, corresponding to the formula $Ln(BANM)_3H_2O$ or $Ln(C_{11}H_{12}Cl_2O_2)_3H_2O$ (where Ln = La, Nd, Sm, Eu, Gd, Dy, Er, and Tm). The complexes are soluble in DMF and DMSO, while molar conductance of the complexes were in the range of 5–8/Ω/cm^2/mol, indicating their non-electrolyte nature (Geary, 1971).

Infrared spectra

The eight rare earth metal complexes were similar in their characteristic infrared absorption peaks as determined by the method of KBr tablet, indicative of their similar structures. In the BANM spectrum, the absorbance of carboxylic group occurred at 1,676 cm^{-1}, while ν_{OH} appeared at ~3,000 cm^{-1} which was identical to the reported spectrum (Sadlter Research Lab. Inc., 1970; Zhang *et al*., 2005). In the spectra of complexes, the peaks at 1,676 cm^{-1} disappeared, and the new peaks were shown around 1574–1577, 1399–1407, and 1521–1514 cm^{-1}, which can be assigned to $\nu_{asy(COO-)}$ and $\nu_{sym(COO-)}$. A different coordination manner of COO^- in metal complexes was reported (Spinner, 1964); IR spectroscopy is a useful tool in diagnosing the nature of carboxylate coordination. The energy difference between $\nu_{asy(COO-)}$ and $\nu_{sym(COO-)}$ is diagnostic of the geometry of carboxylate coordination. Monodentate coordination is

Table 2 Electronic spectral data of Ln(III) complexes

Complex	Bond max (cm^{-1})		S'L'J'	Oscillator strength (10^6)		Bonding parameter
	Nujol	DMSO		Complex	Aqua ion	
$Nd(BANM)_3H_2O$		11,534	$^4F_{3/2}$	12.13	3.02	$\beta = 0.9932$
		12,579	$^4F_{5/2}$	12.13	9.22	$\delta\ \% = 0.6847$
	13,420	13,514	$^4F_{7/2}$,$^2S_{3/2}$	112.15	8.88	$b^{1/2} = 0.0583$
	14,800	14,750	$^4F_{9/2}$	3.04		$\eta = 0.00341$
	16,984	17,182	$^4G_{5/2}$,$^2G_{7/2}$	72.39	10.50	
		19,048	$^4G_{7/2}$	32.75	6.58	
$Er(BANM)_3H_2O$		11,764	$^4I_{9/2}$	41.97	2.37	$\beta = 0.9962$
		15,456	$^4F_{9/2}$	46.28	2.37	$\delta\ \% = 0.0038$
		18,939	$(^2H,^4G)_{11/2}$	71.08	2.91	$b^{1/2} = 0.0436$
		20,618	$^4F_{7/2}$	125.59	2.22	$\eta = 0.0019$

associated with an energy difference of 220–460 cm^{-1}, bridging bidentate coordination with a difference at 140–170 cm^{-1}, and bidentate coordination at 40–80 cm^{-1}, respectively (Nakamoto, 1978; Li *et al*., 2005). In the IR spectra of the complexes, energy differences between $\nu_{asy(COO^-)}$ and $\nu_{sym(COO^-)}$ were ~175 and 60 cm^{-1}; based on this criterion, there were two coordination manners, bridging bidentate and bidentate that existed in the complexes. A dimmer structure involving bridging bidentate and bidentate of COO^- may be tentatively proposed for the rare earth metal complexes. In addition, compared to BANM, the new weak peaks around 498–503 cm^{-1} also appeared in the spectra of the complexes, which can be assigned to ν_{Ln-O} (Zhao *et al*., 2009). The broad band in the spectra of the complexes were observed at 3,365–3,420 cm^{-1} region, which can be assigned to ν_{O-H}; however, water was not involved in coordination as it's other characteristic peaks (600–650 cm^{-1}) did not appear (Sigh *et al*., 1978). The DTA-TG data further supported the conclusion for an endothermic peak that appeared at 86 °C in DTA-TG spectrum of lanthanide complex (2 % mass loss, calc.: 1.91 %), suggesting that water in the complexes was absorption water. No more information could be used to discriminate the coordination mode of BANM.

Electronic spectra

The absorption spectra of the Nd(III) and Er(III) were recorded in the solid (Nujol mull) and in solution (0.01 M in DMSO) state. The spectral data, along with the calculated bonding parameters are included in Table 2. The electronic transitions of the trivalent lanthanides can be of electric-dipole, magnetic-dipole, or electric-quadrupole character; some transitions have appreciable contribution from more than one mode. Electric-dipole transitions within a pure f^N configuration are strictly parity forbidden. However, weak, induced electric-dipole transitions can occur as a result of the interaction of the central ion with the surrounding ligand-field mixing into the f^N configuration states from configuration of opposite parity and thus relaxing the parity restriction. Electric-dipole transitions may also be induced as a result of the asymmetries produced by means of the vibronic coupling of the central ion with its ligands. In contrast to the foregoing electric-quadrupole and magnetic-dipole transition within the f^N configuration parity is allowed. In the Russell–Saunders approximation, magnetic-dipole transitions are restricted by the selection rules (Figgis *et al*., 1960): $\Delta J \leq 1$, $\Delta L = 0$, $\Delta S = 0$, and $\Delta l = 0$. According to the selection rules, some transitions are allowed to appear. Therefore, the weak bands can be seen in higher concentration. In our studied complexes, all the bands show a weak perturbation due to the nephelauxetic effect. The absorption band associated nearly degenerate $^4I_{9/2} \rightarrow {}^2G_{7/2}$, $^4G_{5/2}$ transitions of the Nd(III) ion is well known to exhibit strong hypersensitive behavior (Choppin *et al*., 1966), making it especially suitable for probing the coordinating environment around the metal ion. The hypersensitive band profiles of Nd(III) complex resemble these of the six-coordinated complex $Nd(C_6H_5COCHCOC_6H_5)$ reported by Karraker (Melby *et al*., 1964; Karraker, 1967), indicating that they have similar coordination environment. The absorption intensities were determined experimentally by the area method (Kumer, 1998) and the experimental oscillator strength ($P \times 10^6$) were calculated for the spectral band of the Nd(III) and Er(III) complexes in solution state using the reduced expression (Melby *et al*., 1964):

$$p = 4.318 \times \frac{9\eta}{(\eta^2 + 2)^2} \int \varepsilon(v) \mathrm{d}v$$

where η is the refractive index of the solution, ε is the molar extinction, and v is the energy of the transition. Compared to aqueous metal ion spectra, these values showed an increased trend, which was mostly due to a

lowering of molecular symmetry (Judd, 1966). This was consistent with the result of IR. Various bonding parameters, viz, nephelauxetic ratio (β, bonding parameter ($b^{1/2}$), Sinha's parameter (δ %), and covalency angular overlap parameter (η) were calculated according to literature method (Coutsolelos and Spyroulias, 1994). All these parameters indicate that there were weak covalent bonds between the metals and BANM.

In order to confirm the proposed structure, the dysprosium complex was studied by EPR spectroscopy in frozen solution of DMSO. Only one signal was observed at room temperature in solid state. However, in frozen solution state, the spectrum of the complex exhibited its hyperfine structure with six peaks (DG = 80) at the same time with the peak at the region of free electron (nuclear spin of Dy(III) is 5/2 for both isotopes). The appearance of superhyperfine coupling may be due to the interaction of the free electron with its neighbor atoms and probably the dysprosium (Henrie and Choppin, 1968). The other information was not obtained. Based on the electronic spectrum of Nd(III) complex, and IR spectra, a dimer structure of the complexes can be tentatively proposed as shown in Fig. 2.

The fluorescence spectral characteristics and binding mode

The interaction of the complexes with the Ct-DNA was examined by fluorescence method. The results showed that the fluorescence intensity of the Ct-DNA-EB decreased remarkably with increasing concentration of the complexes added, which indicated that the complexes could bind to Ct-DNA. The fluorescence excitation and emission spectra of the Ct-DNA-EB system in the presence of different concentration of La(III) complex are shown in Fig. 3. The spectral characteristics of the Ct-DNA-EB system in the presence of other complexes were similar. The fluorescence Scatchard plots of EB-Ct-DNA system in the presence of different concentrations of complexes showed that the intercept on both the abscissa (n) and the slope (K_{EB}) decreased with increasing amount of metal complexes. However, the linear relationships of all the Scatchard plots in the presence of different complexes were not good. These results indicated that a complicated binding mode existed between all of the complex and Ct-DNA. The complexes might bind to Ct-DNA with intercalation, electrostatic action, and covalent binding mode (Lepecq and Paotetti, 1967; Howe *et al*., 1976). In general, nitrogen mustards can alkylate the N7 of guanine in DNA. The BANM may also have similar function. The fluorescent intensity decreased profoundly with an increase in the amount of the complexes, indicating that the EB was released from the grooves of DNA due to the cross-linkage of the complexes. The linear relationship may be overall behavior of covalent and electrostatic action, because there is no suitable intercalative group in the complexes. The fluorescence Scatchard plot of the binding of EB to Ct-DNA in the presence of different concentration of La(III) complex is shown as an example in Fig. 4. The n, K_{EB}, and the relative coefficient of the Scatchard plots in the presence of all the complexes are listed in Table 3.

Cytotoxicity effect

The growth inhibitory effects of the BANM and some of its rare earth complexes were examined in Vero and human K_{562} cell lines. Considering the cytotoxicity effect of DMSO, the concentration of DMSO in the medium was controlled below 1 %, so that DMSO did not affect the growth and viability of the cell (DoDodoff *et al*., 1994).

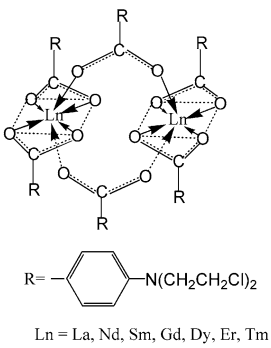

Fig. 2 Tentatively proposed structure of rare earth complexes with BANM

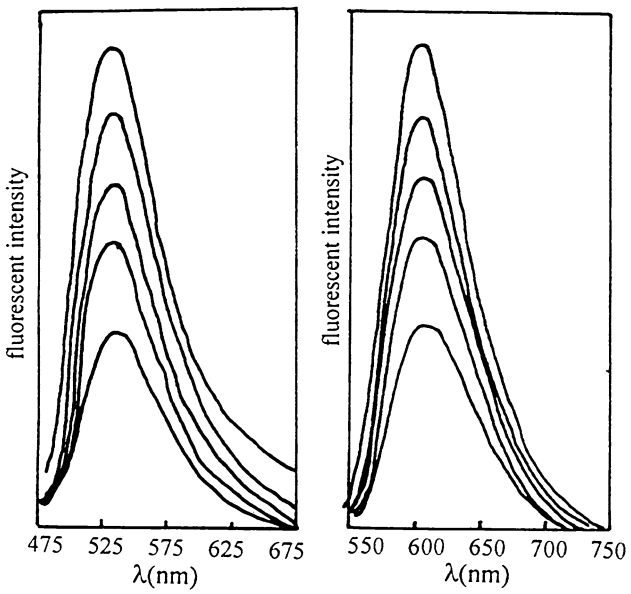

Fig. 3 Effects of the La(III) complex on the fluorescence excitation (*left*) and emission (*right*) spectra of EB-Ct-DNA system. The r (molar ratio of the complex to Ct-DNA) from *top* to *bottom* in the spectra were 0, 2.5, 5, 10, and 15, respectively; the concentration of EB and DNA in phosphorus were kept constant at 4.0×10^{-6} and 4.0×10^{-5} M, respectively

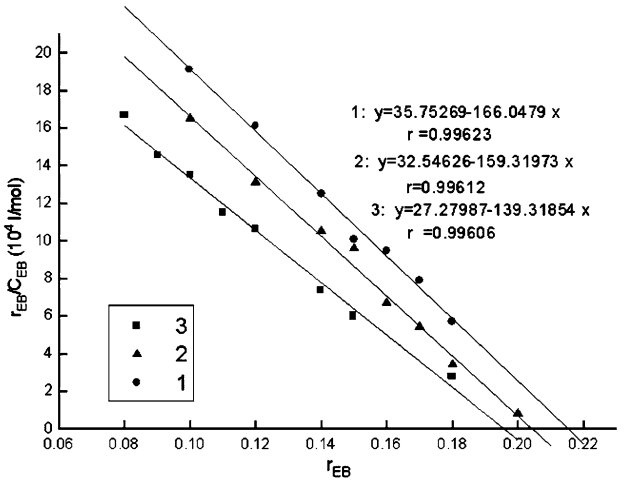

Fig. 4 The fluorescence Scatchard plots of DNA-EB system in the presence of different concentration of La^{3+} complex. Rt increases in the order 0.5, 1.0, and 1.5 for *line* 1–3

Table 3 The characteristics of Scatchard plots of DNA-EB systems in the presence of different concentrations of the complexes

Complex	*R*	Rt	*n*	K_{EB} (10^6/mol/l)
La	0.9962	0.5	0.215	1.66
	0.9961	1.0	0.205	1.59
	0.9960	1.5	0.195	1.39
Eu	0.9915	0.5	0.212	1.67
	0.9876	1.0	0.198	1.60
	0.9891	1.5	0.185	1.51
Dy	0.8973	0.5	0.214	1.65
	0.9125	1.0	0.203	1.57
	0.9000	1.5	0.191	1.42
Sm	0.8865	0.5	0.217	1.64
	0.9011	1.0	0.201	1.58
	0.9201	1.5	0.189	1.50
Gd	0.9073	0.5	0.212	1.66
	0.9121	1.0	0.197	1.58
	0.8992	1.5	0.185	1.49
Tm	0.9215	0.5	0.215	1.62
	0.9300	1.0	0.201	1.56
	0.9179	1.5	0.187	1.41

The results are given in Table 4. It was evident that the BANM had higher antitumor activities against the giving cell lines, and its IC_{50} value is close to the data reported in literature (Anastasiou *et al*., 1994). However, the complexes did not have higher antitumor activity than the BANM did. In general, the complexes in physiological condition may undergo partial dissociation, releasing the active BANM (as electrolyte). However, this situation may not happen partly due to the non-electrolyte nature of the complexes, so the cytotoxicity displayed was probably only

Table 4 Cytotoxicity effect of some compounds (IC_{50} μM)

Compound	Vero	K_{562}
BANM		63
$La(BANM)_3H_2O$	207	131
$Sm(BANM)_3H_2O$	307	157
$Eu(BANM)_3H_2O$	176	220

from the complexes themselves. La(III), Sm(III), and Eu(III) complexes had definite cytotoxicity effect on Vero cell, but less on K_{562} cell line. Normally, the alkylating drugs exhibit their antitumor activities through binding cellular DNA; hence, the ability of passing through cellular membrane is a very important factor. The difference between them in antitumor activities may result from distinct difference in cellular recognition (receptor) or transportation (transporter). In addition, we found that both the BANM and the complexes had different ability causing cellular mutation (data not shown). Compared with positive group (absence of BANM and the complexes), the complexes led to an increase in host cell nucleus larger than that of BANM, which is characteristic of mutation in morphology. It should be noted that although a lot of compounds can interact with DNA via intercalation or alkylation in vitro, the cytotoxicity exhibited by them on cellular level or in vivo was varied significantly, which depends on many factors, such as their permeability through cellular membrane, stability against hydrolases in vivo, and so on. The rare earth metal complexes of BANM displayed less cytotoxic than the ligand, which was beyond our expectation. The difference in cytotoxicity between the complexes and ligand might reflect the difference in manner of crossing membrane, for some metal complexes cross cellular membrane via specific transporter, such as cisplatin, via copper transporter (Howell *et al*., 2010). It is not clear that there is a difference in transportation of BANM and its complexes to crossing cellular membrane, but their distinct cytotoxicity could be overall effects resulting from their interaction with biological components of host cell.

Comet assay

Comet assay has been reported to be a good method of detecting apoptosis, and the amount of DNA damage in the cell was estimated from tail length as the extent of the migration of the genetic material in the direction of the anode (Singh *et al*., 1988). In order to investigate the underlying mechanism, we conducted comet assay. As shown in Fig. 5, in control (Fig. 5, top), non-drug treated cells, the damaged DNA was not detected, and the high-molecular-weight supercoiled DNA remained intact. However, the cells treated

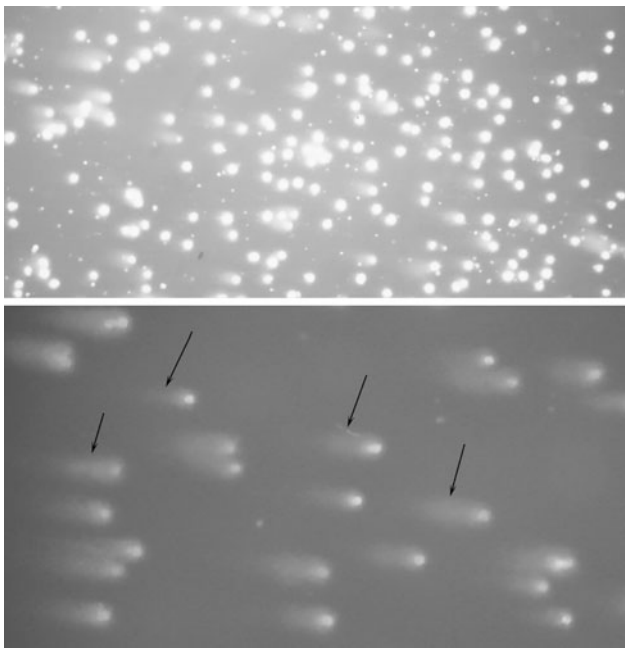

Fig. 5 Typical comet images from K_{562} cells treated with $La(BANM)_3$. *Top part* (untreated as control); and *low part* (treatment with 50 μM followed by 48 h incubation), comet tails were visible as *arrow pointed*. All images stained with EB

with lanthanide complex had a comet tail (Fig. 5, bottom), indicating that the genomic DNA of host cells were broken and fragmentized, which was a general characteristic of apoptotic cell. So we presume that the cytotoxicity exhibited by lanthanide complex may be via interaction (alkylation or intercalation) with cellular DNA, leading to cross-linking of intra or inter-strand of DNA, and initiating apoptosis process. However, the details of the interaction of lanthanide complex with host cell was not clear; a further investigation on apoptotic molecules, such as, how does p53, bcl, bax, or caspases response on mRNA and protein level was required in the future study.

Conclusion

In the present study, BANM and its rare earth metal complexes had been synthesized. The aim was to determine whether the rare earth metals had synergistic effect once forming complexes due to important physiological function of the rare earth metals. Beyond our expectation, the rare earth metal complexes exhibited less cytotoxicity than BANM did. Although the complexes had a definite anti-tumor activity, the metal ions did not display synergistic instead of antagonistic effect once forming complexes with BANM. We presume that the characteristic of non-electrolyte of the complexes may be partial reason for the less cytotoxicity. In addition, the difference in cytotoxicity between the complexes and ligand might reflect the difference in manner of crossing membrane, because some metal complexes cross cellular membrane via specific transporter, such as cisplatin, via copper transporter (Howell *et al*., 2010). It is not clear that there is a difference in transportation of BANM and its complexes, so a deep investigation was required in the future research.

Acknowledgments This study was supported by Xinxiang Medical University (ZD2011-6). The authors would like to thank Dr. qiu-e Cao (Yun Nan University, China) for help in fluorescence experiment.

References

Achyuthan KE, Mary A, Greenberg CS (1989) Tb(III)-ion-binding-induced conformational changes in platelet Factor XIII. Biochem J 257:331–338

Anastasiou A, Catsoulacos P, Papageorgiou A, Margariti E (1994) On the formation of homo-azasteroidal esters of *N*,*N*-bis(2-chloroethyl)aminobenzoic acid isomers and their antitumor activity. J Heterocycl Chem 31:367–374

Beria I, Nesi M (2002) Syntheses of brostallicin starting from distamycin A. Tetrahedron Lett 43:7323–7327

Choppin GR, Henrie DE, Buijs K (1966) Environmental effects on f–f transitions I. Neodymium(III). Inorg Chem 5:1743–1748

Coutsolelos AG, Spyroulias GA (1994) Dysprosium metallation to substituted tetraaryl-porphyrin complexes; synthesis and spectroscopic characterization. Polyhedron 13:647–653

DoDodoff N, Grancharow K, Gugova R (1994) Platinum (II) complexes of benzoic- and 3-methoxybenzoic acid hydrazides. Synthesis, characterization, and cytotoxic effect. J Inorg Biochem 54:221–233

Figgis BN, Lewis J, Wilkins RG (eds) (1960) Modern coordination chemistry. Interscience, New York

Geary WJ (1971) The use of conductivity measurements in organic solvents for the characterisation of coordination compounds. Coord Chem Rev 7:81–122

Gschneidner KA, Jr., LeRoy E (1999) Handbook on the physics and chemistry of rare earths. North-Holland, Amsterdam

Henrie DE, Choppin GR (1968) Environmental effects on f–f transitions. II. "hypersensitivity" in some complexes of trivalent neodymium. J Chem Phys 49:477–482

Howe GM, Wu KC, Bauer WR (1976) Binding of platinum and palladium metallointercalation reagents and antitumor drugs to closed and open DNAs. Biochemistry 15:4339–4346

Howell SB, Safaei R, Larson CA, Sailor MJ (2010) Copper transporters and the cellular pharmacology of the platinum-containing cancer drugs. Mol Pharmacol 77:887–894

Judd BR (1966) Hypersensitive transitions in rare earth ions. J Chem Phys 44:839–840

Karraker DG (1967) Hypersensitive transitions of six-, seven-, and eight-coordinate neodymium, holmium, and erbium chelates. Inorg Chem 6:1863–1868

Koutsourea AI, Fousteris MA, Arsenou ES, Papageorgiou A, Pairas GN, Nikolaropoulos SS (2008) Synthesis, in vivo antileukemic evaluation and comparative study of novel 5-·7-keto steroidal esters of chlorambucil and its active metabolite. In Vivo 22:345–352

Kumer PA (1998) Synthesis and spectral characterization of lanthanide(III) metal complexes of an amino acid hydrazide, *N*-(2-acetyltbiophenoimno)-2-benzamidoethan amide. Synth React Inorg Met-Org Chem 28(5):699–713

Leoni LM, Bailey B, Reifert J et al (2008) Bendamustine (treanda) displays a distinct pattern of cytotoxicity and unique mechanistic features compared with other alkylating agents. Clin Cancer Res 14:309–317

Lepecq JB, Paotetti C (1967) A fluorescent complex between ethidium bromide and nucleic acids: physical—chemical characterization. J Mol Biol 27:87–106

Li C, Wang L, Meng X, Zhao H (1999) Synthesis, characterization and antitumor activity of benzaldehyde nitrogen, mustard picolinoyl hydrazone complexes. Transition Met Chem 24:206–209

Li MX, Shao M, Dai H, An BL, Lu WC, Zhu Y, CX Du (2005) Synthesis and crystal structure of a novel copper(II) complex with acetylenedicarboxylate and 2,2′-bipyridine. Chin Chem Lett 16(10):1405–1408

Li J, Wang L, Bai H, Yang B, Yang H (2011) Synthesis, characterization, and anti-inflammatory activities of rare earth metal complexes of luteolin. Med Chem Res 20:88–92

Melby LR, Rose NJ, Abamson E, Caris JC (1964) Synthesis and fluorescence of some trivalent lanthanide complexes. J Am Chem Soc 68:5117–5125

Nakamoto K (1978) Infrared and Raman spectra of inorganic coordination compounds, 4th edn. Interscience, New York

Nelson DL, Cox MM (2004) Lehninger principles of biochemistry. W. H. Freeman, New York

Qu J, Wang L, Liu Y, Yumin S, Wang Y, Jia X (2006) Syntheses, characterization and antitumour activities of rare Earth metal complexes with 2 (((4,6-dimethyl)-2-pyrimidinyl)thio)-acetic acid. J Rare Earths 24:15–19

Roger GM, Roger FS (1996) Antibody-enzyme conjugates for cancer therapy. J Natl Cancer Inst 88(3/4):153–165

Sadlter Research Lab. Inc. (1970) Sadlter standard Infrared grating spectra, 171162K

Sigh M, Misra SN, Verma RD (1978) Spectral and magnetic properties of lanthanon fluoroacetates. J Inorg Nucl Chem 40:1939–1940

Singh NP, McCoy MT, Tice RR, Schneider EL (1988) A simple technique for quantitation of low levels of DNA damage in individual cells. Exp Cell Res 175:184–191

Spinner E (1964) The vibration spectra of some substituted acetate ions. J Chem Soc 4217–4226

Zhang ZW, Jiang T, Ren SM, Zhang YX, Yu JS (2005) Synthesis, crystal structure and in vitro antitumor activity of di-*n*-butyltin *p*-[*N*,*N*-bis(2-chloroethyl)amino]benzoates. Chin J Chem 23(12): 1655–1758

Zhao L, Chen Y, Zhang H, Li C, Sun R, Yang Q (2009) Study of structure and two-dimension correlation infrared spectroscopy on three rare-earth/3-methylbenzoic acid complexes. J Mol Struct 920:441–449

Zhou M, Fei H, Liu Y, Li WF (2010) Metal complexes and their applications in bioassay bio-imaging and protein staining. Prog Chem 22(1):201–209